Cement & Concrete Composites 34 (2012) 493–502

Contents lists available at SciVerse ScienceDirect

Cement & Concrete Composites

journal homepage: www.elsevier.com/locate/cemconcomp

Creep of UHPC in tension and compression: Effect of thermal treatment

V.Y. Garas [1], K.E. Kurtis *, L.F. Kahn

School of Civil and Environmental Engineering, Georgia Institute of Technology, Atlanta, GA, USA

ARTICLE INFO

Article history:
Received 28 June 2011
Received in revised form 30 November 2011
Accepted 3 December 2011
Available online 16 December 2011

Keywords:
Design
Interface
Fibers
Prestressed concrete
Thermal treatment
Ultra-high performance concrete

ABSTRACT

Steel fiber-reinforced ultra-high performance concrete (UHPC) is of increasing interest for use in precast prestressed concrete highway bridge girders due to its superior durability and the potential for reducing or eliminating shear reinforcement, due to the presence of steel fibers. However, the contributions of creep, and especially tensile creep, to long-term performance must be better understood to develop appropriate design specifications. Due to practical considerations, it is also of interest to investigate the influence of varying thermal treatment, including temperatures lower than those recommended by the manufacturer (i.e. 90 °C), on the creep of UHPC. In this 1-year study, the effects of three different thermal treatment regimes on tensile and compressive creep performance of UHPC are examined, with complementary characterization by nanoindentation and scanning electron microscopy. Results show that UHPC creeps phenomenologically differently in tension and compression. Both thermal treatments examined resulted in similar tensile creep behavior, suggesting that a lower temperature applied over a longer period could effectively cure UHPC. For the non-thermally cured UHPC, a 10 μm wide region observed at the fiber/matrix interface was characterized by reductions in elastic modulus as well as greater porosity and microcracking than the bulk paste. It is suggested that the quality of the fiber/matrix interface is a major contributor to the measured increased creep of non-thermally treated UHPC as compared to UHPC treated at 60 °C or 90 °C.

1. Introduction

Ultra-high performance concrete (UHPC) is of increasing interest for precast prestressed concrete highway bridge girders because it has the potential to reduce maintenance costs associated with steel and conventional concrete girders. Commonly, steam curing beds in precast concrete plants are designed for temperatures not in excess of 70 °C (158 °F), to avoid delayed ettringite formation (DEF) in concrete [1]. This practice presents a challenge for the mass-production of ultra-high performance concrete (UHPC) structural elements, where thermal treatment at 90 °C (194 °F) is required by the producer of the UHPC "premix". A recent study has confirmed that the application of thermal treatment at 90 °C (194 °F) to UHPC for 48 h significantly improved almost all material properties investigated [2]. Further, several studies have shown that the application of thermal treatment to concrete, and specifically UHPC, can activate silica fume (and perhaps other materials), resulting in a net reduction in the pore size which improves the cementitious matrix structure and performance [3,4]. However, changing thermal processing temperatures in casting plants presents a cost to the plant. Therefore, it is of interest to better understand the implications of varying thermal processing on the structure and long-term performance of UHPC.

Furthermore, prior studies have suggested that the short steel fibers typically used in UHPC mixes may serve as shear reinforcement, similar to stirrups in bridge girders [5–10]. However, the long-term behavior of inclined (shear) cracks induced by diagonal tension near girder supports in the absence of stirrups has not been investigated. That is, it is unknown whether UHPC girders without conventional stirrups will creep in tension to failure, and it is unknown what reliability factor should be applied to the diagonal tension capacity of UHPC in bridge structures.

While some studies have examined tensile creep behavior in ordinary and high performance concrete [11–20], tensile creep of UHPC has not been well-characterized in the published literature. A preliminary study by the authors [21] used short-term tensile creep studies to demonstrate that steel fiber reinforcement and thermal treatment can limit deformation in UHPC, but concluded that further evaluation is necessary to better understand the underlying mechanisms of tensile creep in UHPC. Here, the effect of two thermal treatment regimes in addition to ambient curing on tensile creep performance is examined through testing and characterization. Tensile creep behavior is compared to compressive creep results to determine if past compressive creep studies

* Corresponding author. Address: 790 Atlantic Dr., Atlanta GA 30332-0355, USA. Tel.: +1 404 385 0825; fax: +1 404 894 2278.
E-mail addresses: kk92@ce.gatech.edu, kkurtis@ce.gatech.edu (K.E. Kurtis).
[1] Present address: Offshore Function, ExxonMobil Upstream Research Company, Houston, TX, USA.

0958-9465/$ - see front matter © 2011 Elsevier Ltd. All rights reserved.
doi:10.1016/j.cemconcomp.2011.12.002

may be relied upon for improved understanding of tensile phenomena. The traditional creep tests were augmented using scanning electron microscopy and nanoindenation to better understand the processes involved in tensile creep and, in particular, the influence of the quality of the bond between the fibers and the UHPC matrix. This research is necessary to better understand tensile creep in UHPC and for the development of design criteria for UHPC in highway bridge girders.

2. Experiment

The experimental program in this study includes testing of UHPC mixtures under varying thermal treatment conditions. All the mixtures designs were identical and were based on the UHPC manufacturer's recommendation; they all included steel fibers at 2% volume fraction. In addition, they were all mixed and cast following the procedure outlined in [21,22].

2.1. Materials, mix design, and casting

The UHPC mixes investigated were prepared from ultra-high performance premix, Ductal® (Lafarge North America) and ultra-high strength steel fibers (Bekaert's Dramix 13/0.20), using the proportions given in Table 1. According to the manufacturer, the UHPC premix consisted mainly of portland cement, silica fume, crushed quartz, and sand. The high strength steel fibers were 0.20 mm (0.008 in.) in diameter and 13.0 mm (0.51 in.) in length (aspect ratio = 65), with a tensile strength of between 690 and 1000 MPa (96,600 and 140,000 psi) and a modulus of elasticity of 210,000 MPa (30,457 ksi), according to the manufacturer. Also, commercially available polycarboxylate high range water reducer (HRWR, Lafarge's Premia 150) was used. Mixing was performed in an 85-L capacity high shear mixer (Eirich R08W) at 30–35 rpm, following procedures described in [21,22].

Three 75 × 75 × 483 mm (3 × 3 × 19-in) tensile creep specimens and three companion free shrinkage prism specimens of the same dimensions were cast for each thermal treatment case. In addition, two 100 × 380 mm (4 × 15-in.) compressive creep cylinders and one companion free shrinkage cylinder were cast for each case. Tensile and compressive creep specimens for a given thermal treatment condition were cast of the same batch. All specimens were poured horizontally from one end to the other resulting in fiber alignment, as would be expected during casting operations in commercial facilities [23].

2.2. Thermal treatments

Three different curing regimes, depicted in Fig. 1a, were examined. The 90 °C regime (Fig. 1a) follows UHPC manufacturer's recommended heat treatment at 90 °C (194 °F) at ~100% RH, starting at the age of 48 h and continuing for an additional 48 h. The 60 °C regime (Fig. 1b) represents thermal treatment conditions that can be achieved in most of US casting plants, with heat treatment applied at the age of 48 h and continued for 72 h at 60 °C (140 °F) at

Table 1
UHPC composition.

Constituent	kg/m^3 (lb/ft^3)
UPHC premix	2194 (137)
Water	109 (6.80)
HRWR	31 (1.94)
Steel fibers	156[1] (9.74)

[1] Dose recommended by the UHPC manufacturer (2% volume fraction).

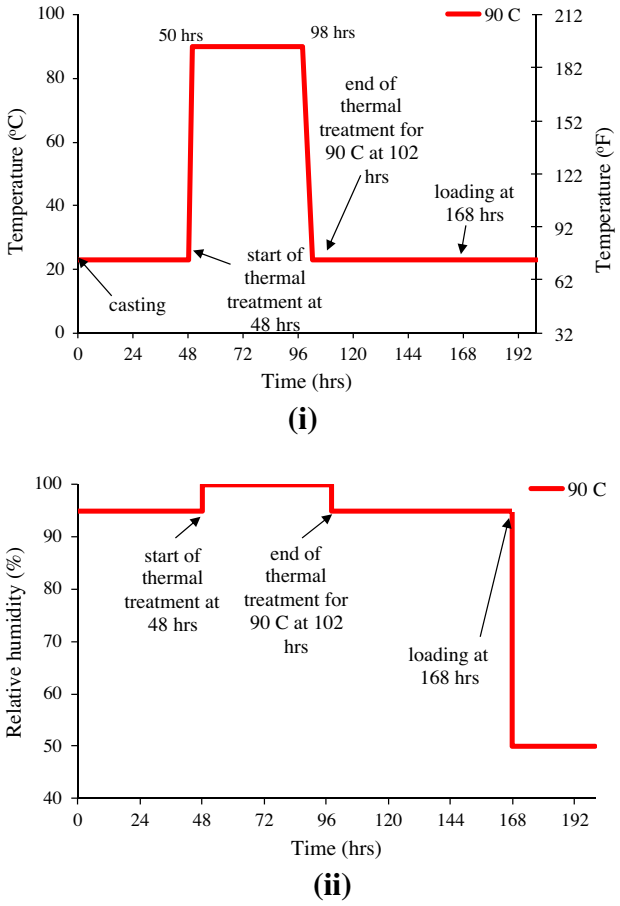

Fig. 1a. 90 °C (194 °F) curing regime (i) temperature and (ii) relative humidity.

100% RH using steam curing. The third regime (Fig. 1c) represents field curing at ambient temperature (i.e. 23 °C (73 °F)). It should be noted that the total heat input applied during thermal treatment regime 2 (at 60 °C) is equal to the manufacturer's recommended practice of thermal treatment at 90 °C, due to the longer duration of heat application at the lower temperature.

Table 2 summarizes the tensile creep test specimens, their curing and tensile loading. The nomenclature used in this study was based on the type of UHPC used (i.e., Ductal® = D), fiber volume fraction (i.e., 2% volume fraction = 2f), maximum treatment temperature reached (i.e. 23 °C, 60 °C or 90 °C (73 °F, 140 °F or 194 °F)), and the stress-to-strength level maintained during the creep test (e.g., 40% means that the applied stress to strength ratio at the time of loading was 40%). For the compressive creep test, the letter "C" is added after the letter "D" to differentiate between tensile and compressive creep cases. Shrinkage and strength test specimens show no loading stress-to-strength ratio.

2.3. Testing for mechanical properties

After initial curing or initial curing plus thermal treatment, three direct tension and five compression tests were performed for each UHPC mix just before the start of creep tests to obtain tensile strength and modulus and compressive strength and modulus, respectively, for each case. Table 3 summarizes the mechanical tests performed at 7 days, in advance of the creep testing. Details about the direct tension test performed are found in a previous study [24]. Analysis of variance (ANOVA) results showed no significant difference between the compressive modulus of elasticity values for mixes D-2f-90C-40 and D-2f-60C-40.

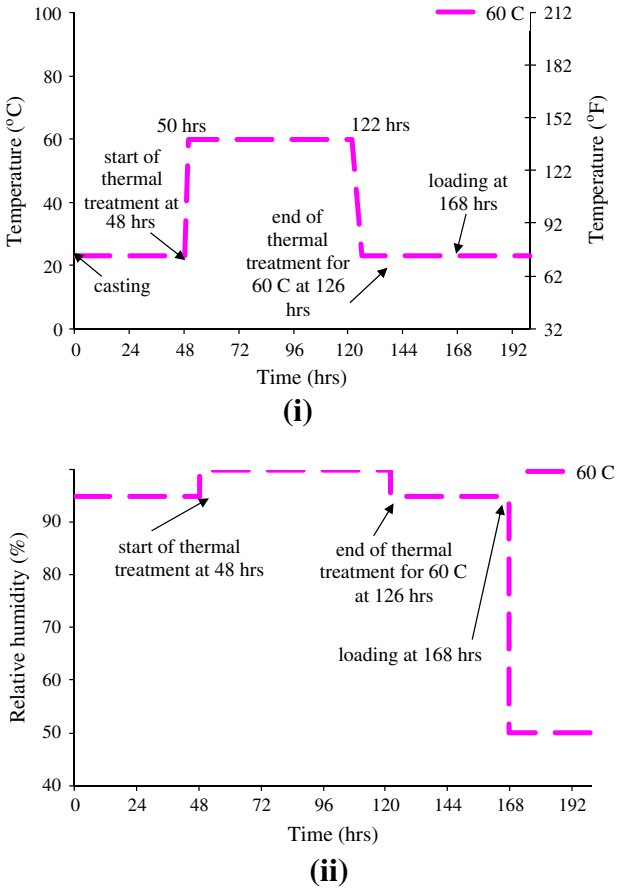

Fig. 1b. 60 °C (140 °F) curing regime (i) temperature and (ii) relative humidity.

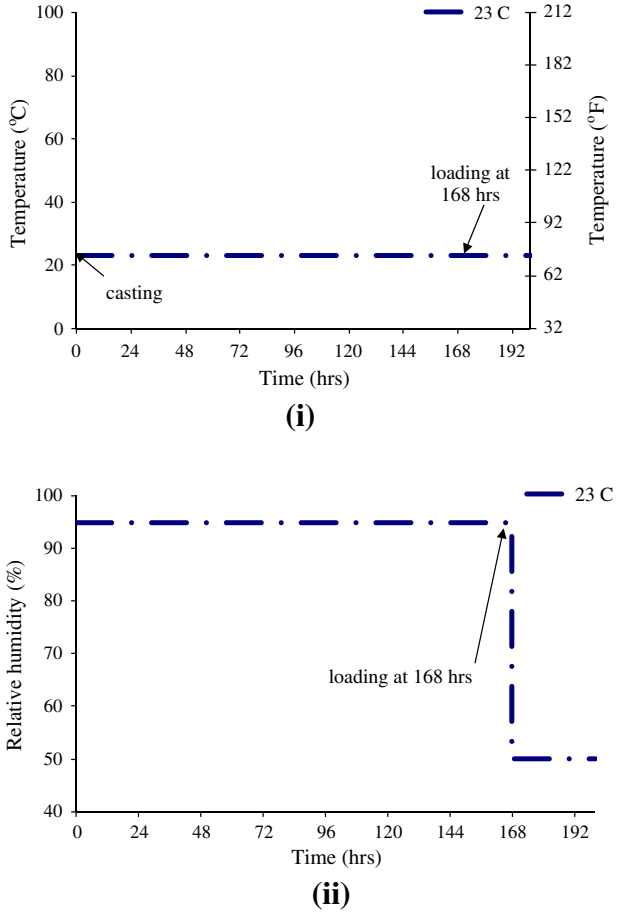

Fig. 1c. 23 °C (73 °F) curing regime (i) temperature and (ii) relative humidity.

2.4. Creep and shrinkage testing

The tensile creep test setup and procedure used has been described in a previous study [24], but a brief description is provided here. Fig. 2 shows the tensile creep specimen dimensions, with steel end plates and embedded bolts of different lengths to avoid excessive stress concentrations. The design of test frames was inspired by a tension creep test developed by Bissonnette and Pigeon [14]. However, this design was modified for increased load capacity up to 6800 kg (15,000 lbs) and testing of three 75 × 75 × 483 mm (3 × 3 × 19-in.) UHPC concrete prisms, with four measurements of deformation per specimen. Tensile loads were applied by hanging weights at the end of the dead load lever-arm via a metal ball knob that kept the threaded rod connecting the dead loads to the loading arm, always in a vertical position. The dead load magnification factor was 10. That is, a 1 lb. applied dead load is magnified through the lever-arm to apply 10 lbs. load to the tensile creep specimens, for example.

All samples were loaded at 40% of their measured direct tensile strength at 7 days. Conditions were kept at 23 °C ± 2 °C (73 °F) and 50 ± 3% RH for the entire testing period. Tensile creep deformations were measured initially at 1, 2, 4, 6, and 24 h after loading. Subsequently, measurements were made daily for 1 week, weekly for a month, and monthly for a year. Two prisms identical to the creep specimens were stored adjacent to the creep specimens and were used to measure drying shrinkage. Strain data were collected at the same times as creep data. Specific creep was calculated by dividing the adjusted tensile creep strain by the initial applied stress. The adjusted tensile creep strain ("creep strain") is equal to the algebraic sum of the measured total creep strains and the free shrinkage strains.

Compressive creep of each UHPC mixes shown in Table 2 was measured on three 100 × 380 mm (4 × 15-in.) cylinders according to ASTM C 512 specifications [25]. The size of the specimens used in this study is different from the ASTM C 512 standard (150 × 300 mm (6 × 12-in.)). This modification was necessary due to the high strength of UHPC which dictated a reduction in cross section. (The cylinders used for measuring compressive creep here had the same surface area-to-volume ratio, 1, as the cylinders used in another study by Graybeal [2].) All cylinders were instrumented with four sets of steel inserts located on diametrically opposite surfaces of each specimen. Each set of inserts had a 10-in. (254-mm) long gauge length for measuring deformation with a detachable mechanical gauge (DEMEC gauge). After appropriate thermal treatment (Table 2), compressive creep tests started age of 7 days of age, where the applied load was equivalent to 40% of the 7-day strength for each thermal treatment condition.

Specific creep was calculated by dividing the adjusted creep strain by the initial applied stress. The adjusted creep strain was calculated by subtracting the shrinkage strain, measured on unloaded companion samples, from the measured total creep strains.

2.5. Sample characterization

UHPC samples for characterization by nanoindentation and scanning electron microscopy (SEM) were cast in 30 mm (1.2 in.) diameter cylinders with depth of ~12 mm (1/2 in.). All samples were cast and cured following similar procedures identical to the large-scale study described above, with the exception of the method of fiber addition. After casting non-fiber reinforced UHPC into

Table 2
UHPC mixes, thermal treatment and loading conditions.

Mixture ID	Stress/strength at loading (%)	Thermal treatment temperature[a]
D-2f-90C-40	40	90 °C (194 °F)
D-2f-60C-40	40	60 °C (140 °F)
D-2f-23C-40	40	23 °C (73 °F)
D-C-2f-90C-40	40	90 °C (194 °F)
D-C-2f-60C-40	40	60 °C (140 °F)
D-C-2f-23C-40	40	23 °C (73 °F)
D- 2f-90C	N/A	90 °C (194 °F)
D-2f-60C	N/A	60 °C (140 °F)
D-2f-23C	N/A	23 °C (73 °F)

[a] All samples were cured or thermally treated at relative humidity between 95% and 100%.

the molds, 16 steel fibers pre-fixed on a plastic sheet in a square configuration were pushed vertically into the middle 5 × 5 mm (0.2 × 0.2-in.) region of the specimen to create a 2% fiber volume fraction in this region similar to that of the creep specimens. After curing or curing and thermal treatment, fast setting epoxy was poured on the top surface of the specimens to cover the top ends of fibers and also to provide more support to fibers during polishing. The bottom surfaces of the samples were then prepared by successive dry polishing as outlined by Mondal et al. [26]. Complete details on sample preparation are provided in [21,22].

Nanoindentation was performed under displacement control using a pyramid shaped, diamond Berkovich tip with a nominal radius of 50 nm, an elastic modulus, E_{in}, of 1100 GPa (159,542 ksi), and a Poisson's ratio, υ_{in}, of 0.07. Prior to performing the nanoindentation test, successive calibrations of the indents' locations were performed. Indentations were performed from the fiber into the matrix along four lines in orthogonal orientation to one another, with indentation spacing of 2 μm (79 μin.). A spacing-to-indentation depth ratio of 20 was used to assure that no overlap would occur between successive indents.

After sputter coating with gold, SEM imaging was performed on the indented samples. SEM was carried out using a LEO 1530 thermally-assisted field emission (TFE) scanning electron microscope at low pressure 10^{-7} Pa (1.45 ksi). The accelerating voltage was 10 kV. Characterization was performed in secondary electron mode to better distinguish the surface features.

3. Results and discussion

The influence of varying thermal treatment was assessed in free shrinkage and creep studies performed on UHPC for 1 year. Because the thermal treatments produced significant increases in compressive and tensile strengths (Table 3), it is important to note that for the creep testing, the load applied was proportional to the strength at the time of application (7 days). In addition, Table 3 shows that for both cases of thermal treatment, the moduli of elasticity were also higher than for specimens with no thermal treatment. To better understand the processes involved particularly in tensile creep, UHPCs subjected to each of the thermal treatments were characterized by scanning electron microscopy and nanoindenation, in addition to long-term creep results presented herein. Such a multi-scale approach allows for improved understanding of the complex structure–property relationships involved in creep of UHPC.

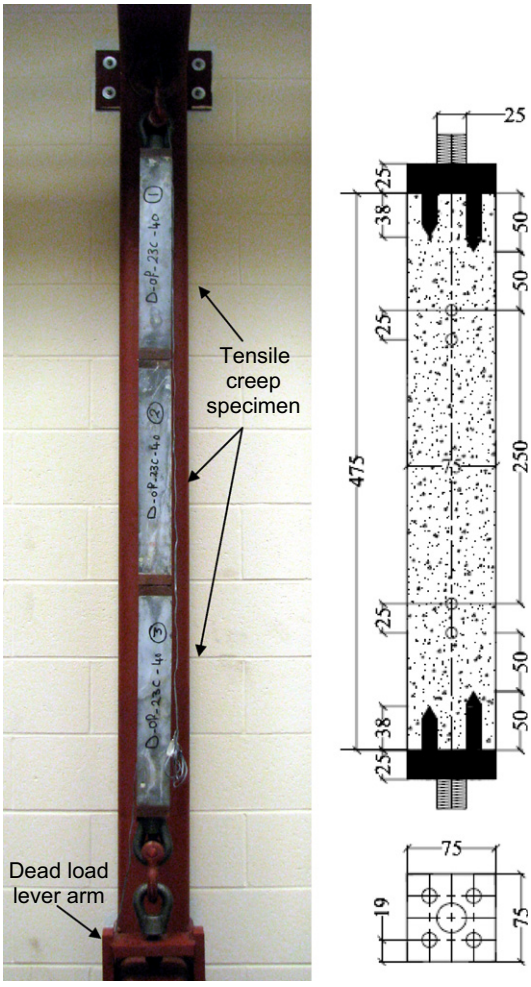

Fig. 2. Tensile creep specimens in mm.

Table 3
Summary of 7-day mechanical properties of UHPC subjected to various curing regimes.

	Compressive strength MPa (ksi)	Tensile strength MPa (ksi)		Modulus of elasticity MPa (ksi)	
		Splitting tension	Direct tension	E_c	E_t
Sample dimensions, mm (in.)	75 × 150-mm (3 × 6-in.) cylinders	75 × 150-mm (3 × 6-in.) cylinders	235 mm (9.25-in.) dogbones, 50 × 50 mm (2 × 2-in.) mid-length cross section	100 × 200-mm (4 × 8-in.) cylinders	235 mm (9.25-in.) dogbones, 50 × 50 mm (2 × 2-in.) mid-length cross section
Standard	ASTM C 39	ASTM C496	–	ASTM C 469	–
Replicates	5	5	3	3	3
Mixture ID					
D-2f-90C-40	169 (24.6)	22 (3.2)	10.3 (1.5)	47,950 (6953)	57,470 (8336)
D-2f-60C-40	148 (21.4)	19 (2.8)	9.7 (1.4)	50,870 (7376)	58,060 (8420)
D-2f-23C-40	116 (16.9)	16 (2.3)	7.5 (1.1)	44,900 (6510)	56,810 (8241)

3.1. Tensile creep and shrinkage

Figs. 3 and 4 show 1-year data for free shrinkage, and specific tensile creep of UHPC subjected to varying thermal treatment, and key results are summarized in Table 4. Compared to UHPC thermally-treated at 90 °C for 48 h, thermal treatment at 60 °C for 72 h and eliminating thermal treatment resulted in 13% and 172% increase in specific tensile creep, respectively. Also, compared to UHPC thermally-treated at 90 °C for 48 h, results showed an increase of 28% and 260% in the free shrinkage strain with thermal treatment at 60 °C for 72 h and eliminating thermal treatment, respectively, after 1 year of drying.

Based on the mean values reported in Tables 3 and 4, the effect of thermal treatment was more pronounced on the tensile creep deformation than on the tensile strength. For example, a 173% increase occurred in specific creep versus a 27% decrease in tensile strength upon eliminating thermal treatment. This observation underscores that tensile creep testing, rather than tensile strength values at the time of loading, should be used to predict long-term tensile performance. It is proposed that the ability of pre-existing cracks to coalesce and propagate during long-term creep testing rather than short-term strength test likely plays an important role in the difference between creep results and tensile strength results.

From a practical point of view, long-term tensile creep results along with the mechanical test data suggest that the magnitude of thermal energy applied to UHPC is a more critical factor in developing the microstructure than the method in which this energy is applied, as long as the thermal treatment is applied beginning 2 days after casting as in this case. This observation is of specific practical importance as it suggests that satisfactory UHPC mixes can be achieved at moderate thermal treatment temperatures that can be reached in most of the existing concrete precasting facilities.

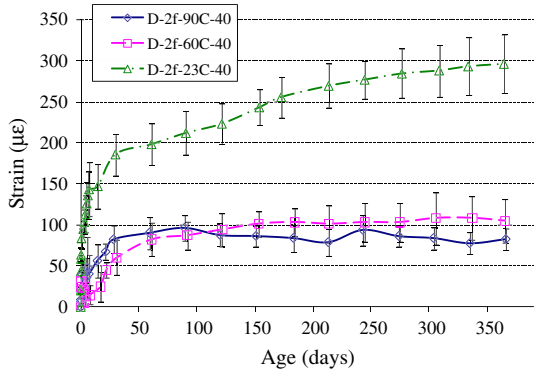

Fig. 3. Effect of thermal treatment on free shrinkage strain.

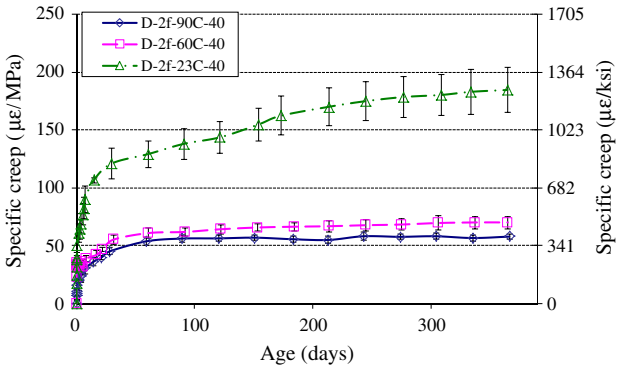

Fig. 4. Effect of thermal treatment on specific tensile creep.

Table 4
Summary of UHPC tensile creep and shrinkage measured at 1 year.

Mix	Free shrinkage strains at 1 year (με)	Specific tensile creep at 1 year με/MPa (με/ksi)
D-2f-90C-40	82	54 (372)
D-2f-60C-40	105	64 (443)
D-2f-23C-40	296	176 (1216)

Table 5
Maturity adjusted ages of UHPC at the time of testing (7 days).

Mix	Temperature adjusted age at 7 days (days)	Equivalent age at 7 days (days)
D-2f-90C-40	33.94	38.26
D-2f-60C-40	20.12	24.80
D-2f-23C-40	8.02	13.11

This observation emphasizes also the dependency of tensile creep on the maturity of concrete at the time of loading. Thermal treatment, along with internally generated heat (due the high cementitious fraction and increased particle fineness common in UHPC), are expected to result in increases in equivalent age (or maturity) for UHPC, particularly at early ages. While the dependence of creep on maturity has been known [27], just one creep model, CEB-FIP model [28,29], explicitly incorporates temperature history at the time of loading [30]:

$$t_e = t_{0,T} \cdot \left(\frac{9}{2 + t_{0,T}^{1.2}} + 1 \right)^{\alpha} \geq 0.5 \tag{1}$$

$$t_{0,T} = \sum_i \Delta_i \cdot \exp - \left\{ \frac{4000}{273 + T(\Delta t_i)} - 13.65 \right\} \tag{2}$$

where t_e is the equivalent age (days), $t_{0,T}$ the temperature adjusted age (days), T (Δt) the temperature during the interval Δt_i (°C), Δt_i the period of time at temperature T (days), and α is the parameter depending on the type of cement (−1 for slowly hardening cement, 0 for normal and rapid hardening cement, and 1 for rapid hardening high strength cement).

Assuming that the internal temperature of the UHPC creep samples was the same as the temperature in the curing environment (Figs. 1a–1c), the equivalent age was calculated from the temperature history of each mixture and stage using Eqs. (1) and (2), where rapid hardening cement was assumed.

Results in Table 5 and Fig. 5 show a clear inverse relationship between the maturity at the time of loading and the ultimate tensile creep achieved. Also, results in Fig. 5 shows a pronounced reduction in slope between the two thermally-treated systems (curing at 60 °C (140 °F) and 90 °C (194 °F)), as compared to the slope between the non-thermally treated UHPC and UHPC thermally treated at 60 °C (140 °F). This observation has an important practical impact as it allows for modification to the method of thermal treatment by decreasing the maximum temperature and increasing the treatment time to achieve satisfactory long-term tensile performance.

3.2. Compressive creep and shrinkage

Results from this 1-year study of free shrinkage (Fig. 6) and specific compressive creep (Fig. 7) showed a significant influence of the curing conditions prior to loading on the shrinkage and compressive creep performance (Table 6). Compared to UHPC ther-

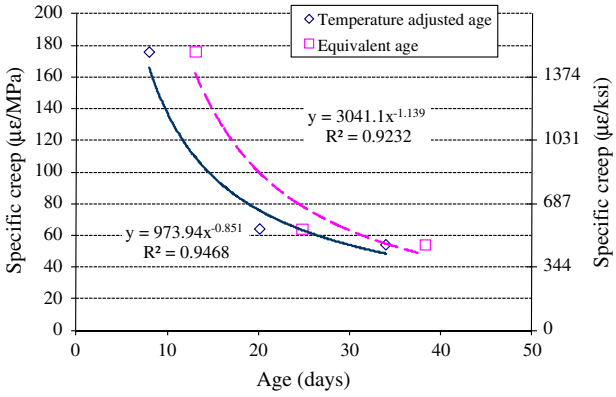

Fig. 5. Correlations between the ultimate tensile creep after 1 year and the maturity level of UHPC at the time of loading.

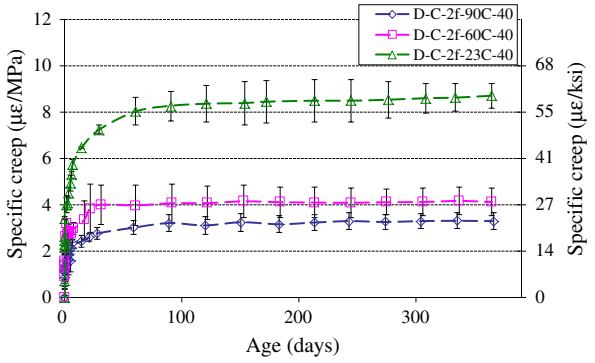

Fig. 7. Effect of thermal treatment on specific compressive creep.

mally-treated at 90 °C for 48 h, thermal treatment at 60 °C for 72 h prior to loading resulted in a 10% and 24% increase in the creep strain and the specific compressive creep, respectively. Also, eliminating thermal treatment resulted in an 81% and 163% increase in the creep strain and the specific compressive creep compared to UHPC thermally-treated at 90 °C for 48 h prior to loading. These percentage increases in specific compressive creep upon altering the thermal treatment regime or eliminating thermal treatment were much larger than decreases in compressive strength (Table 2) resulting from either modification. That is, thermal treatment of fiber reinforced UHPC at 60 °C for 72 h prior to loading resulted in a 12% decrease in compressive strength while eliminating thermal treatment of UHPC resulted in a 31% decrease in compressive strength compared to UHPC thermally-treated at 90 °C for 48 h prior to loading.

In addition, results showed an increase of 28% and 266% in the free shrinkage strain after 1 year of drying with thermal treatment at 60 °C for 72 h and eliminating thermal treatment compared to UHPC thermally-treated at 90 °C for 48 h. Also, it can be seen that the effect of thermal treatment on reducing free shrinkage was similar for prisms and cylinders used in this study.

For compressive creep, Graybeal [2] reported 1-year specific creep of 5.7 με/MPa (39 με/ksi) for a mix very similar to D-C-2f-90C-40; that is ~70% greater than the value reported here. In the prior study, a similar 41% stress level was applied but at 4 days, rather than at 7 days as here. This difference in specific creep between the two studies may be in part attributed to the difference in the equivalent ages (i.e., 31.14 versus 38.26 days) between the two experiments. Also, differences in casting procedures between the current and the previous studies may have contributed to these differences. That is, in the current study, the molds were horizontal, and the UHPC was poured into the molds from one end to the other which allowed fiber alignment in the longitudinal (loading) direction and which simulated field methods for casting UHPC bridge girders. This was not the case in where the cylinder molds were oriented vertically, and the molds were filled from the top, as is commonly done in testing labs [2].

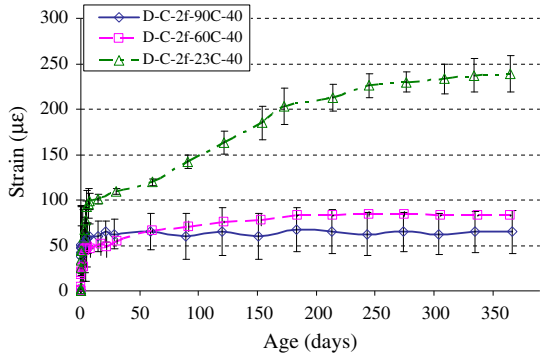

Fig. 6. Effect of thermal treatment on free shrinkage strain.

Table 6
Summary of compressive creep and shrinkage properties of UHPC at 1 year.

Mix	Free shrinkage strains at 1 year (με)	Specific compressive creep at 1 year με/MPa (με/ksi)
D-C-2f-90C-40	65	3.3 (22.6)
D-C-2f-60C-40	83	4.1 (28.5)
D-C-2f-23C-40	238	8.7 (59.8)

Vertical placement of UHPC results in more random fiber orientation, as shown in Fig. 8. The image at the right clearly shows an increase in fibers aligned longitudinally in the case of the 100 × 380 mm (4 × 15-in.) specimens used in the current study. It is expected that an increased number of fibers oriented in the loading direction could then result in increased deformation in that direction. Crane [23] has recently shown that alignment of fibers in UHPC girders can have significant influences on structural performance. Thus, it is recommended that future studies employ casting techniques which best replicate conditions in practice.

3.3. Comparison between tensile and compressive creep

The main objective in comparing tensile and compressive creep results for the three UHPC mixtures was to better understand the mechanisms affecting tensile creep of UHPC. It was necessary to adjust the tensile creep results to account for differences in specimen geometry between the tensile and compressive creep studies. This adjustment was possible because the same specimen geometry used in the long-term compressive creep study presented here had been used in a prior short-term (~340-h) study for tensile creep by the authors [21]. This allowed adjusting the long-term tensile creep and shrinkage results based on the specific creep and shrinkage strain results after 7 days obtained for mix D-2f-90C-40. That is, results from the long-term tensile creep and shrinkage D-2f-90C-40, D-2f-60C-40, and D-2f-23C-40 were multiplied by a calculated specific creep and shrinkage strain short-term-to-long-term ratio. Adjusted long-term tensile creep and shrinkage will be referred to as "adjusted tensile creep" and "adjusted shrinkage".

The short-term-to-long-term ratio for mix D-2f-90C-40 was 1.05 and 1.00 for specific creep and for free shrinkage, respectively, resulting in no adjustment to the long-term shrinkage data and

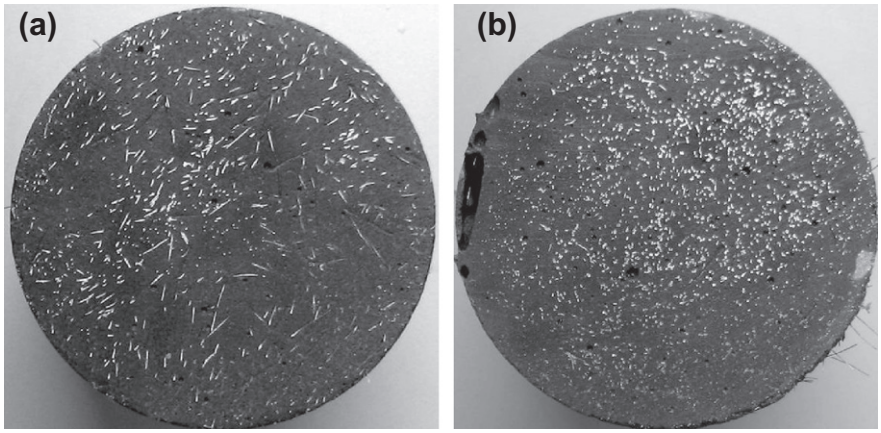

Fig. 8. Cross-sectional images at mid-height of (a) 100 × 200 mm cylinder poured vertically from the top and (b) 100 × 380 mm cylinder poured horizontally from one end to the other.

adjusted long-term specific tensile creep shown in Fig. 9. The small difference between the short and the long-term specimens is in part due to shape and size effects.

Comparing compressive creep to adjusted tensile creep, show that, except for mix D-2f-90C-40, tensile creep continues to increase after 1 year, while compressive creep has reached an asymptotic value. Comparing adjusted tensile creep results to compressive creep results also shows that the tensile creep of mixes D-2f-90C-40, D-2f-60C-40, D-2f-23C-40 was about 17, 16, and 18 times the measured compressive creep, respectively. These large differences suggest that these phenomena occur in fundamentally different ways.

3.4. Characterization by nanoindentation and SEM

It is well-known that defects (e.g., voids, microcracks) in brittle materials like concrete have a more pronounced influence on behavior in tension than in compression [31]. Therefore, the order of magnitude increase in tensile creep compared to compressive creep suggests that these defects, which are likely to be present in increased proportions at an interface such as that between the fibers and paste in UHPC, have an important effect on the tensile creep performance of UHPC. This hypothesis was further examined through nanoindentation and scanning electron microscopy (SEM), which were performed to better understand (1) the role of defects, particularly those which may be present at the fiber/matrix interface and (2) the influence of each of the thermal treatment regimes.

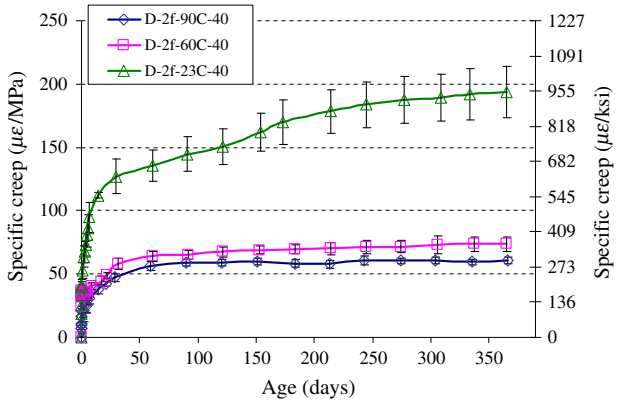

Fig. 9. Adjusted specific tensile creep.

Fig. 10 shows the indentation pattern implemented across the fiber–matrix interfacial zone, extending from the steel fiber surface into the surrounding matrix, in a non-thermally-treated specimen. It can be seen in Fig. 10 that debonding or cracking at the fiber/paste interface is apparent in this sample, as is a zone approximately 2–3 μm (79–118 μin.) wide of unreacted cementitious particles, which are apparent because of their relative brightness.

From nanoindentation performed in an orthogonal pattern, with indents extending from the fiber through the fiber/cement interface and into the bulk paste, variation in the modulus of elasticity with increasing distance from the fiber edge for each of the three curing conditions are shown in Fig. 11. All modulus values were calculated from the unloading indentation curves. The modulus of elasticity for the bulk paste (i.e., determined away from fiber edge) in mix D-2f-90C ranged between 38.7 GPa (5613 ksi) and 57.2 GPa (8296 ksi) with an average of 47.6 GPa (6904 ksi). This average modulus of elasticity of mix D-2f-90C is just ~1% less than the static compressive modulus of elasticity for mix D-2f-90C-40 (Table 3), showing good agreement between the modulus determined by nanoindentation and standard compression testing. The average modulus of elasticity obtained here is also in good agreement with nanoindentation modulus values obtained by Sorelli et al. [32], where the average modulus value for UHPC thermally treated at 90 °C (194 °F) was found to be 49.4 GPa (7225 ksi). The modulus of elasticity for mix D-2f-60C ranged between 40.2 GPa (5825 ksi) and 50.4 GPa (7304 ksi) with an average of 45.6 GPa (6608 ksi). This average modulus of elasticity of mix D-2f-60C is about 10% less than the static compressive modulus of elasticity for this case (Table 3); the lower value measured by nanoindentation will require further examination, as the relatively low variation in modulus values measured particularly near the fiber interface suggests that defects at the interface are not prevalent in D-2f-60C. The elastic moduli measured in the D-2f-90C case also do not show the influence of any defects that may be present in that region. And, although ANOVA revealed significant difference between the modulus of elasticity of the two thermally cured cases, the similarity of the modulus results from the nanoindentation study are in good agreement with the similarity of the creep results obtained for these two cases (Figs. 4 and 7).

In contrast, Fig. 11 shows relatively larger variations in the modulus of elasticity values for mix D-2f-23C, where the average modulus measured was 23 GPa (3365 ksi). The modulus values are at a local minimum adjacent to the fiber and generally increase within the 20 μm closest to the fiber. The values remain relatively inconsistent across the 70 μm distance interrogated. It is proposed that this variation is related to defects present in the microstructure in the interfacial zone. For example, localized high porosity

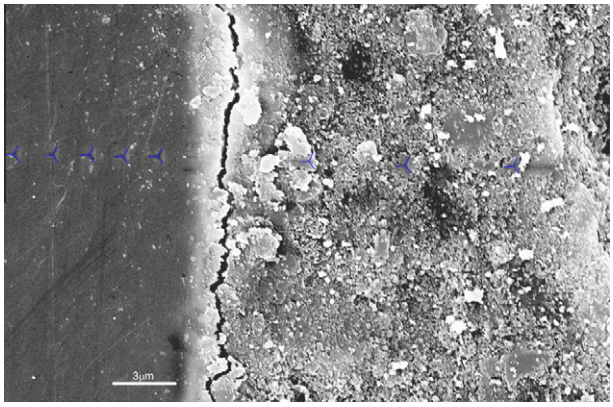

Fig. 10. Indentation pattern at the fiber–matrix interfacial zone of a non-thermally treated specimen. Indent spacing was 2 μm, and indents are more clearly apparent in the steel than in the paste. When clearly apparent, indent locations have been marked.

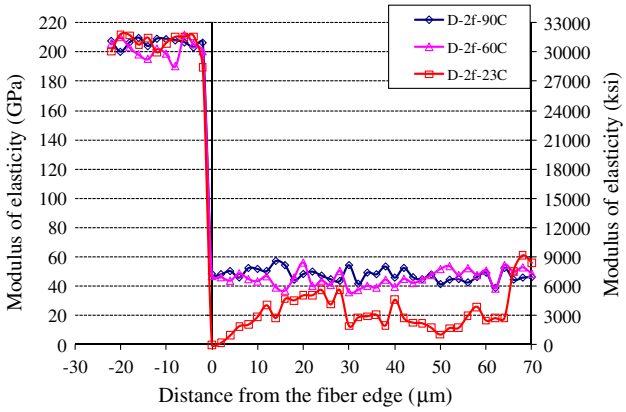

Fig. 11. Variation in elastic modulus with distance from fiber edge for each of the three thermal treatment cases.

or debonding around the fibers is evident in the 4 μm (157 μin.) adjacent to the fibers where the average modulus of elasticity measured was zero. As the distance from the fiber edge increased beyond 4 μm (157 μin.), the modulus of elasticity values increased, reaching 26.9 GPa (3902 ksi) at a distance of about 10 μm (394 μin.) from the fiber edge; this value was maintained for about another 50 μm (1969 μin.) away from the fiber (i.e. up to a distance of 60 μm (2362 μin.)), and then modulus values started to increase to about 55 GPa (7977 ksi) at a distance of 70 μm (2756 μin.) from the fiber edge. As a result, a more porous interface can be defined in this case by a 10 μm (394 μin.) wide annulus around the fibers.

Characterization of UHPC subjected to each of the three thermal treatment regimes also shows differences in the microstructure at the fiber/cement interface (Fig. 12). The presence of a porous zone around the fiber in the non-thermally treated case was suggested by nanoindentation data and was confirmed via SEM scans carried out at the same locations as the indentations. The size of the porous zone, 10 μm (394 μin.), suggested by nanoindentation data is in good agreement with SEM images. SEM also showed no such porous zone for either of the thermally treated cases, in agreement with characterization of thermally-treated UHPC by a previous study [32]. It is proposed that this increased densification in the paste and lack of voids or cracking may be attributed to the thermal treatment, which could promote further reaction of the cementitious paste, leading to increased density (and decreased porosity) around the fibers.

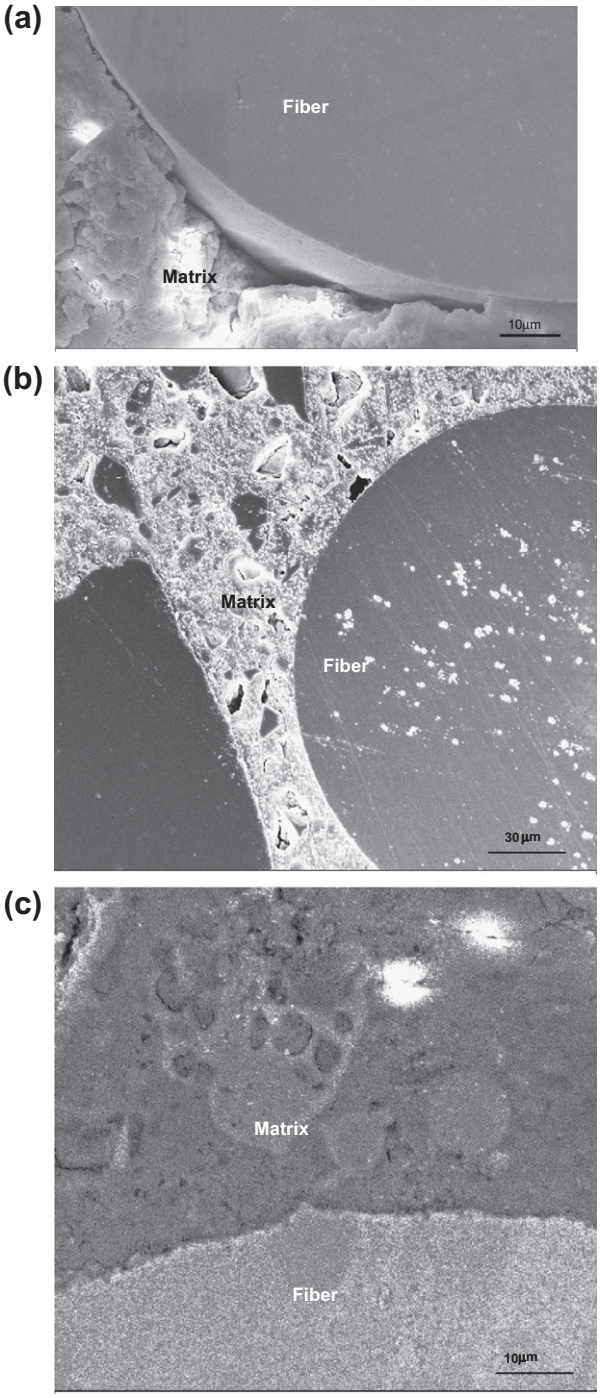

Fig. 12. SEM micrographs, all at 3000x magnification, at the fiber/matrix interface for (a) D-2f-23C, (b) D-2f-60C, and (c) D-2f-90C.

3.5. Contributions of defects to tensile creep of UHPC

The current multi-scale investigation suggests that microcracking, here observed at the fiber/matrix interface, can be a major factor affecting tensile creep of UHPC. The microcracking effect on creep was introduced by Neville and Dilger [27] for compressive creep of concrete and was adopted later by Bissonnette et al. [20] to explain tensile creep. However, no microstructural evidence was provided in these prior studies. Here, nanoindentation data and SEM images show the presence of a more porous and more poorly bonded fiber/matrix interfacial region in the non-thermally cured samples. The significance of these defects can be seen both by comparing

the tensile creep behavior of thermally treated and non-thermally treated UHPCs and also by comparing the tensile to the compressive creep behavior of all mixes investigated.

Characterization by SEM and nanoindentation showed that steel fibers in non-thermally treated UHPC were surrounded by a porous interface that may contain pre-existing cracks. The weak bond between fibers and the cementitious matrix in non-thermally treated UHPC would result in limited stress transfer to fibers. Tensile cracks are likely to propagate and grow interconnected under tension stress due to stress concentrations occurring at the crack tips [27]. Each of these cracks is likely to propagate until growth is arrested by a fiber present in the crack path(s). Once microcrack growth is locally arrested by a fiber, a decrease in the tensile creep rate can be expected. It is then proposed that in non-thermally treated UHPC the failure of fibers to adequately arrest microcracks – due to the weak bond at the interface – resulted in the continuous increase in tensile creep after 1 year; in comparison, compressive creep, where stress concentrations at the crack tip would be expected to be less than in the case of tensile creep, reached almost an asymptotic value after 150 days.

4. Conclusions

A comprehensive investigation of tensile and compressive creep of fiber-reinforced UHPC was presented. Based on this experimental investigation, an improved understanding of the influence of thermal treatment on the creep behavior of UHPC is gained and the following conclusions can be drawn:

(1) Tensile creep of UHPC was found to be more sensitive to thermal treatment compared to tensile strength. The direct tensile strength with no thermal treatment was 7.5 MPa at 7 days while that with 90 °C treatment was 10.3 MPa, a 37% increase. The specific tensile creep in UHPC with no thermal treatment was 176 με/MPa at 1 year while that with 90 °C treatment was 54 με/MPa, a 69% decrease.

(2) Large scale tensile creep tests showed that thermal treatment of UHPC at 90 °C (194 °F) for 48 h or at 60 °C (140 °F) for 72 h prior to loading decreased specific tensile creep by about 63% and 57%, respectively, when compared to non-thermally treated UHPC.

(3) The closeness of the tensile creep behavior for the two thermally treated UHPC mixes investigated suggests the possibility of achieving satisfactory microstructural refinement if the same temperature energy is input to UHPC despite of the maximum temperature applied.

(4) The specific compressive creep with no thermal treatment was 8.3 με/MPa at 1 year while that with 90 °C treatment was 3.3 με/MPa, a 60% decrease. The thermal treatment at 60 °C and 90 °C significantly decreased compressive creep, although the compressive strength increased from 116 to 169 MPa, 46%.

(5) Results from this study suggest that the tensile creep phenomenon in UHPC occurs differently than compressive creep. This result emphasizes the importance of further study of the tensile creep behavior of UHPC, particularly for applications where satisfactory long-term tensile performance is required.

(6) For the first time, the presence of a more porous fiber-cementitious matrix interface, about 10 μm (394 μin.) wide, was demonstrated by nanoindentation and scanning electron microscopy, for the case of the non-thermally treated UHPC only. No porous interface was found in thermally treated UHPC, in either the 90 °C or 60 °C curing regimes.

(7) It is proposed that microcracking and porosity, including those at the fiber/matrix interface, can markedly affect tensile creep of fiber-reinforced UHPC. Further research is needed to fully describe the factors affecting the tensile creep phenomenon in concrete.

Acknowledgements

This work was sponsored by the Georgia Department of Transportation under Research Project No. 2043. The opinions and conclusions expressed in this study are those of the authors and do not represent the opinions, conclusions, policies, standards or specifications of the Georgia Department of Transportation. Lafarge North America's support of this research through donating the UHPC premix is gratefully appreciated.

References

[1] Taylor HFW, Famy C, Scrivener KL. Delayed ettringite formation. Cem Concr Res 2001;31(5):683–93.
[2] Graybeal BA. Characterization of the behavior of ultra-high performance concrete. PhD thesis, University of Maryland; 2005.
[3] Richard P, Cheyrezy M. Reactive powder concretes with high ductility and 200-800 MPa compressive strength. ACI international conference on concrete technology past, present and future SP 144; 1995.
[4] Feylessoufi A, Crepin M, Dion P, Bergaya F, Van Damme H, Richard P. Controlled rate thermal treatment of reactive powder concretes. Adv Cem Mater 1997;6(1):21–7.
[5] Narayanan R, Darwish IYS. Shear in prestressed concrete beams containing steel fibres. Int J Cem Compos Lightweight Concr 1987;9(2):81–90.
[6] Imam M, Vandewalle L, Mortelmans F, Van Gemert D. Shear domain of fibre-reinforced high-strength concrete beams. Eng Struct 1997;19(9):738–47.
[7] Furlan Sydney Jr, Hanai JB. Shear behaviour of fiber reinforced concrete beams. Cem Concr Compos 1997;19(4):359–66.
[8] Furlan Sydney Jr, Hanai JB. Prestressed fiber reinforced concrete beams with reduced ratios of shear reinforced. Cem Concr Compos 1999;21(3):213–21.
[9] Lim DH, Oh BH. Experimental and theoretical investigation on the shear of steel fibre reinforced beams. Eng Struct 1999;21(10):937–44.
[10] Cucchiara C, Mendola LL, Papia M. Effectiveness of stirrups and steel fibers as shear reinforcement. Cem Concr Compos 2004;26(7):777–86.
[11] Umehara H, Uehara T, Iisaka T, Sugiyama A. Effect of creep in concrete at early ages on thermal stress. In: Springenschmid R, editor. Thermal cracking in concrete at early age. E&FN Spon, London, RILEM; 1994. p. 79–86.
[12] Gutsch A, Rostasy, FS. Young concrete under high tensile stresses, creep, relaxation and cracking. In: Springenschmid R, editor., Thermal cracking in concrete at early age. E&FN Spon, London, RILEM; 1994. p. 111–8.
[13] Kovler K. Testing system for determining the mechanical behavior of early age concrete under restrained and free uniaxial shrinkage. J Mater Struct 1994;27(6):324–30.
[14] Bissonnette B, Pigeon M. Tensile creep at early ages of ordinary, silica fume and fiber reinforced concretes. Cem Concr Res 1995;25(5):1075–85.
[15] Kovler K. Interdependence of creep and shrinkage for concrete under tension. ASCE J Mater Civil Eng 1995;7(2):96–101.
[16] Kovler K. A new look at the problem of drying creep of concrete under tension. ASCE J Mater Civil Eng 1999;11(1):84–7.
[17] Kovler K, Igarashi S, Bentur A. Tensile creep behavior of high strength concretes at early age. J Mater Struct 1999;32(5):;383–387.
[18] Altoubat SA, Lange DA. Tensile basic creep: measurements and behavior at early age. ACI Mater J 2001;98(5):386–93.
[19] Tao Z, Weizu Q. Tensile creep due to restraining stresses in high-strength concrete at early ages. Cem Concr Res 2006;36(3):584–91.
[20] Bissonnette B, Pigeon M, Vaysburd AM. Tensile creep of concrete: study of its sensitivity to basic parameters. ACI Mater J 2007;104(4):360–8.
[21] Garas VY, Kahn LF, Kurtis KE. Short-term tensile creep and shrinkage of ultra-high performance concrete. Cem Concr Compos 2009;31(3):147–52.
[22] Garas VY. Multi-scale investigation of tensile creep of ultra-high performance concrete for bridge applications. PhD thesis, Georgia Institute of Technology; 2009.
[23] Crane CK. Shear and shear friction of ultra-high performance concrete bridge girders. PhD thesis, Georgia Institute of Technology; 2010.
[24] Garas VY, Kahn LF, Kurtis KE. Tensile creep test for concrete: performance of fiber-reinforced ultra-high performance concrete. ASTM J Test Eval 2010;38(6):1–9.
[25] ASTM C512. Standard test method for creep of concrete in compression. Philadelphia, Pennsylvania. American Society for Testing and Materials; 2002.
[26] Mondal P, Shah SP, Marks LD. Nanoscale characterization of cementitious materials. ACI Mater J 2008;105(2):174–9.

[27] Neville AM, Dilger WH. Creep of concrete: plain, reinforced, and prestressed. Amsterdam. New York: North-Holland Pub. Co., American Elsevier; 1970. xix: 622.
[28] Comite Euro-Internacional du Beton (CEB) and Federation Internationale de la Precontrainte (FIP). Evaluation of the time dependent behavior of concrete. Lancaster: The Construction Press; 1990.
[29] Comite Euro-Internacional du Beton (CEB) and Federation Internationale de la Precontrainte (FIP). CEB code final draft section 3 materials 1992-1; 2001. p. 25–31.
[30] Lopez M. Creep and shrinkage of high performance lightweight concrete: a multi-scale investigation. PhD thesis, Georgia Institute of Technology; 2005.
[31] Mehta PK, Monteiro PJM. Concrete microstructure, properties, and materials. 3rd ed. McGraw-Hill; 2005.
[32] Sorelli L, Constantinides G, Ulm FJ, Toutlemonde F. The nano-mechanical signature of ultra high performance concrete by statistical nanoindentation techniques. Cem Concr Res 2008;38(12):1447–56.